

# Three-dimensional structural analysis of the morphological condition of the alveolar bone before and after orthodontic treatment

Yasuhiro Shimizu  
Takashi Ono

Division of Oral Health Sciences,  
Department of Orofacial Development  
and Function, Graduate School, Tokyo  
Medical and Dental University, Tokyo,  
Japan

Assessing the condition of the alveolar bone before and after orthodontic treatment is important. Recently, cone-beam computed tomography has been widely accepted as a useful tool for orthodontic treatment. Moreover, using a three-dimensional (3D) structural analysis software enables gathering detailed information and quantifying data. The aim of this study was to introduce various quantitative analyses performed before and after orthodontic treatment by using a 3D structural analysis software for evaluating the morphological condition of the alveolar bone of a patient with gingival recession around the canines.

[Korean J Orthod 2017;47(6):394-400]

**Key words:** Computed tomography, Three-dimensional structural analysis, Alveolar bone

Received December 28, 2016; Revised April 4, 2017; Accepted May 16, 2017.

**Corresponding author:** Yasuhiro Shimizu.

Part-time Lecturer for Orthodontic Science, Division of Oral Health Sciences, Department of Orofacial Development and Function, Graduate School, Tokyo Medical and Dental University, 1-5-45 Yushima, Bunkyo-ku, Tokyo 113-8549, Japan.

**Tel** +81-3-5803-5528 **e-mail** [y.shimizu.orts@tmd.ac.jp](mailto:y.shimizu.orts@tmd.ac.jp)

The authors report no commercial, proprietary, or financial interest in the products or companies described in this article.

© 2017 The Korean Association of Orthodontists.

This is an Open Access article distributed under the terms of the Creative Commons Attribution Non-Commercial License (<http://creativecommons.org/licenses/by-nc/4.0>) which permits unrestricted non-commercial use, distribution, and reproduction in any medium, provided the original work is properly cited.

## INTRODUCTION

Inflammation, swelling, and recession in the gingiva sometimes occur around the tooth in conditions of occlusal hypofunction, for example, in the case of a high-displaced canine.<sup>1-3</sup> The deteriorating gingival effect is caused by atrophic changes in collagen metabolism in the periodontal ligament and alveolar bone. Indeed, several studies have shown that alveolar bone resorption is accelerated, whereas bone formation is suppressed in conditions of occlusal hypofunction.<sup>4-8</sup>

Recently, cone-beam computed tomography (CBCT) has been widely accepted as a useful tool for orthodontic treatment.<sup>9-11</sup> Moreover, using a three-dimensional (3D) structural analysis software enables gathering detailed quantitative information. However, to date, this analysis technique has been exclusively used in animal experimental models, including rodents.<sup>6-8</sup>

In the present report, we introduce 3D quantitative analyses of the alveolar bone before and after orthodontic treatment to evaluate the morphological condition of the human alveolar bone.

## ETIOLOGY AND DIAGNOSIS

### Etiology

The patient was a man aged 60 years and 1 month, whose chief complaint was anterior crowding because of arch length insufficiency.

### Diagnosis

The patient had a straight profile, Class I molar relationship, and a normal mandibular plane angle (the ANB angle [ANB] = 1.6°; the Frankfort-mandibular plane angle [FMA] = 22.2°) (Figure 1A). Gingival recession around the canines was confirmed (Figure 1B). Intraoral examination revealed an overjet of +1.0 mm, and overbite of +1.0 mm (Figure 1B).

## TREATMENT OBJECTIVES

The treatment objectives were to eliminate crowding. Careful treatment planning was essential to avoid the gingival recession observed on CBCT. CBCT images for evaluating the bone condition were acquired immediately before orthodontic treatment and at 1 year after active treatment, because some reports have suggested that relapse usually occurs within a few months

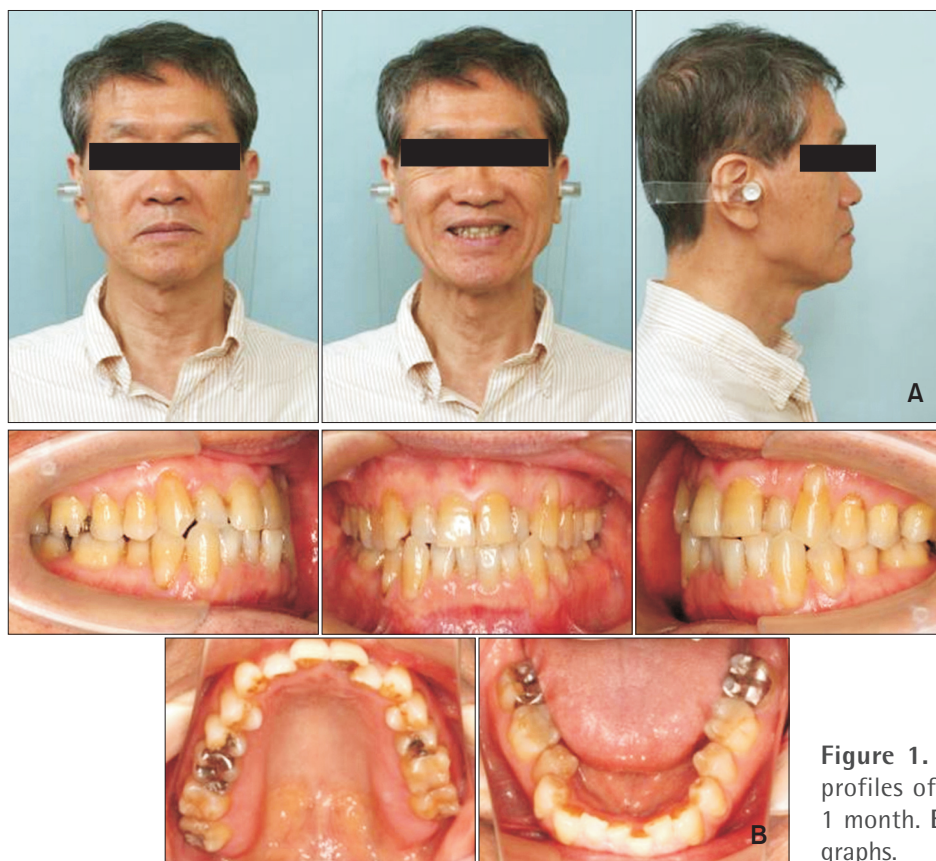


**Figure 1.** A, Pretreatment frontal/lateral profiles of the patient aged 60 years and 1 month. B, Pretreatment intraoral photographs.

to 1 year after active treatment.<sup>12-15</sup> CBCT was performed using 3D Accuitomo FPD8 (Morita Corp., Kyoto, Japan) with an image intensifier. The field of view was 80 × 80 mm and the voxel size was 0.16 × 0.16 × 0.16 mm. We analyzed the adaptive threshold level to exclude the cortical/trabecular bone from the bone marrow according to the instructions provided by the manufacturer of the 3D image analysis software (TRI/3-D-BON; Ratoc System Engineering, Tokyo, Japan) and by using the discriminant analysis method.<sup>16</sup> We then divided the enamel and bone by applying the same method using the 3D image analysis software.<sup>16</sup> The study participants provided informed consent, and the study design was approved by the ethics review board of the Tokyo Medical and Dental University (permission numbers, 846 and 1254).

### TREATMENT ALTERNATIVES

If we expanded the dental arch to eliminate crowding, the canines could protrude from the buccal alveolar bone base because CBCT revealed the alveolar bone surrounding the canine was thin in this patient. Thus, we tried not to expand the dental arch, but to make an

interproximal reduction to eliminate crowding.

### TREATMENT PROGRESS

The premolars and molars, but not the maxillary and mandibular incisors, were bonded using 0.018 × 0.025-inch (in) slot preadjusted edgewise brackets (Roth-type prescription). To aid leveling with a light continuous force, a 0.014-in improved superelastic nickel-titanium alloy wire (ISW) (SENTALLOY-Medium; Tomy, Tokyo, Japan) followed by a 0.016 × 0.022-in ISW (L&H Titan, Tomy) was placed. We performed orthodontic stripping from the initial stage on the interproximal surfaces between the canines (i.e., approximately 3.0 mm in total) in both the maxilla and the mandible.

After gaining space for the anterior discrepancy, both the maxillary and mandibular incisors were bonded using 0.018 × 0.025-inch slot preadjusted edgewise brackets. The active treatment period was 2 years and 3 months.

For retention, the patient was instructed to wear removable retainers for 24 hours a day for the first year, and at night only for the next year. Occlusal rest for the right maxillary third molar was incorporated into the upper retainer to prevent overeruption.

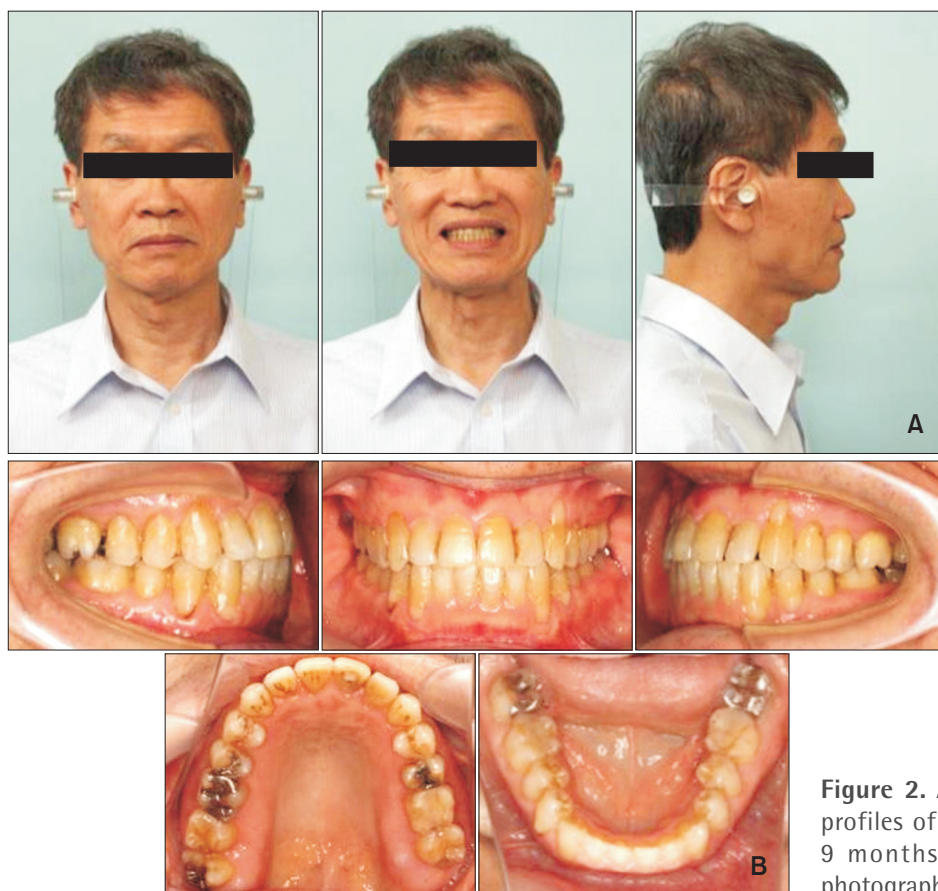


**Figure 2.** A, Posttreatment frontal/lateral profiles of the patient aged 62 years and 9 months. B, Posttreatment intraoral photographs.

## RESULTS

The anterior crowding was eliminated without gingival recession after active treatment (Figure 2). The change in maxillary and mandibular intercanine widths was from 36.0 mm to 36.5 mm and from 36.5 mm to 36.5 mm, respectively. This indicated that the treatment could successfully avoid gingival recession and alveolar bone resorption surrounding the maxillary and mandibular teeth.

First, we examined the cortical bone before orthodontic treatment. The region of interest (ROI) was the buccal side of the canines, and the result of bone volume analysis before treatment showed that the cortical bone surrounding the right mandibular canine was lower than that in the other three quadrants (Figure 3A–3C). Three-dimensional images of the cortical bone were constructed using a micro-CT analysis software (TRI/3-D-BON) according to methods described in the literature.<sup>6–8</sup> We analyzed the adaptive threshold level to exclude the bone from the bone marrow according

to the instructions provided by the manufacturer of the 3D image analysis software by using the discriminant analysis method; we also divided the enamel and bone by using the same method.<sup>16</sup> We measured the percentage of bone volume per tissue volume (BV/TV, %) and the connectivity of the cortical bones (mm<sup>3</sup>), which indicated the mean volume of the bone as measured in all directions from a particular point inside the bone (Figure 3C).

Furthermore, we examined the trabecular bone around the canine root. The ROI was 1.28 mm around the apex of the root, and we constructed the 3D images by using the micro-CT analysis software (Figure 4A and 4B). The percentage of BV/TV, trabecular thickness (Tb.Th, mm), trabecular number (Tb.N, per mm), marrow space star volume (Vm, mm<sup>3</sup>), and trabecular star volume (Vtr, mm<sup>3</sup>) were measured. The marrow space star volume (Vm) indicates bone rarefaction. The trabecular star volume (Vtr) indicates connectivity of the trabecular bone.<sup>17–19</sup> The trabecular bone parameters showed an improvement in the rarefaction of bone tendency after

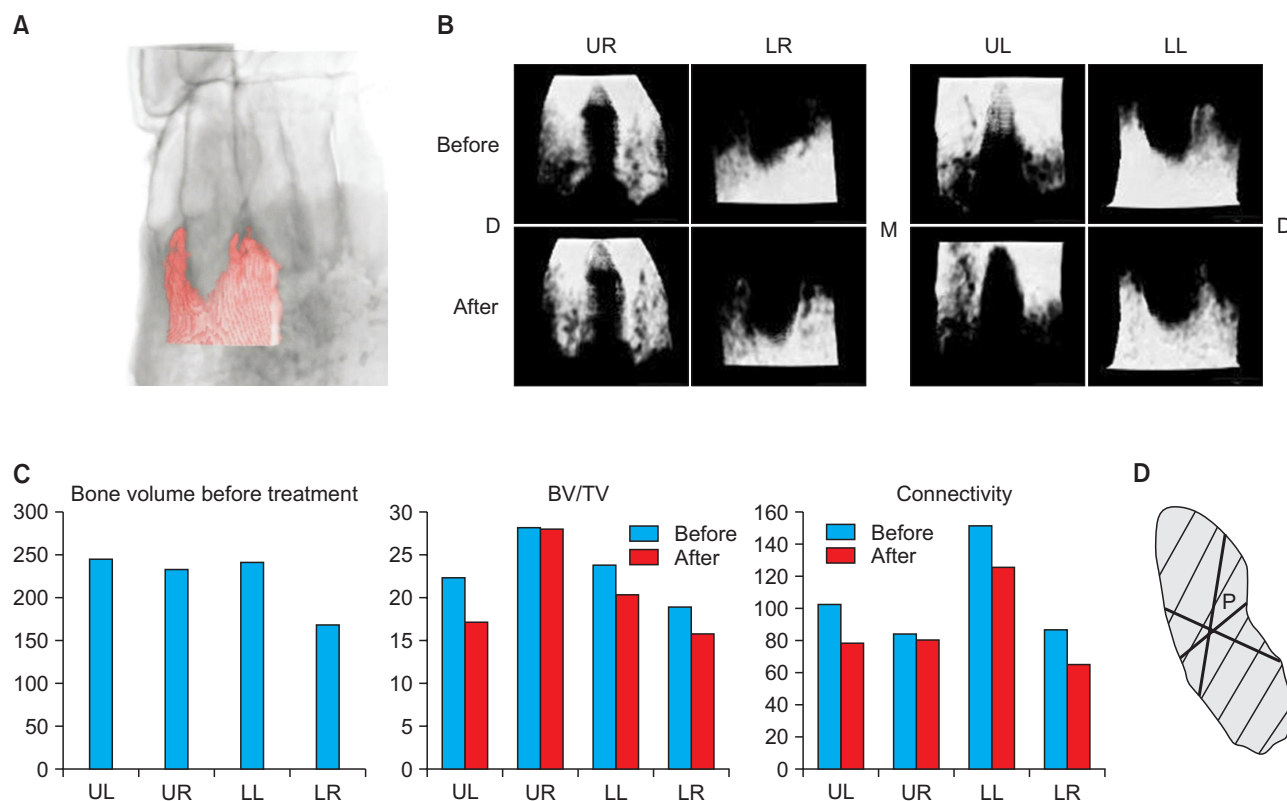


**Figure 3.** A, Cortical bone surrounding the lower canine (red area). B, Three-dimensional reconstructed images of the cortical bone surrounding the canines. C, The bone volume before treatment, bone volume per tissue volume (BV/TV), and connectivity of the cortical bones before/after treatment. Blue bar, before treatment; red bar, after treatment. D, Diagram of “connectivity,” which is defined as the average volume from the point in the trabecular bone to the end of the trabecular bone in all directions. The shaded area, bone; P, a point. UL, Upper left; UR, upper right; LL, lower left; LR, lower right; M, medial; D, distal.

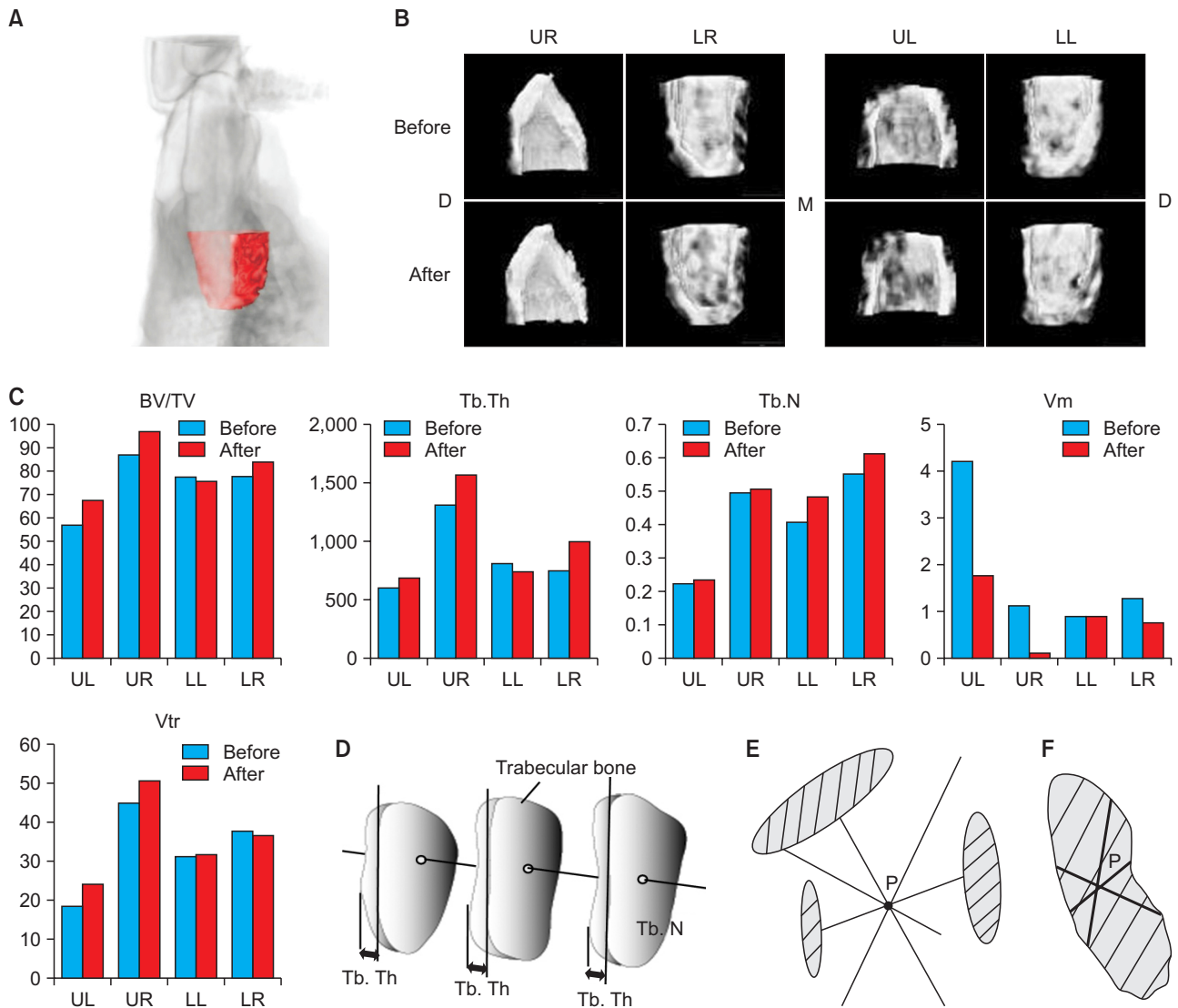


**Figure 4.** A, Trabecular bone surrounding the lower canine (red area). B, Three-dimensional reconstructed images of the trabecular bone surrounding the canines. C, The bone volume per tissue volume (BV/TV), trabecular thickness (Tb.Th, mm), trabecular number (Tb.N, per mm), marrow space star volume (Vm, mm<sup>3</sup>), and trabecular star volume (Vtr, mm<sup>3</sup>) before/after treatment, and a diagram of those parameters. Blue bar, before treatment; red bar, after treatment. D, Diagram of Tb.Th and Tb.N. E, Diagram of Vm. F, Diagram of Vtr. The shaded area, bone; P, a point. UL, Upper left; UR, upper right; LL, lower left; LR, lower right; M, medial; D, distal.

the orthodontic treatment (Figure 4C), which may be in line with previous findings regarding the changes caused by an occlusal hypofunctional condition.<sup>4-8</sup>

Stability of retention was evaluated after 2 years, and the evaluations revealed no significant gingival recessions and relapse.

### DISCUSSION

In animal experimental models, we have examined the alveolar bone microstructure by using micro-

CT analysis.<sup>6-8</sup> Using a 3D structural analysis software enables gathering detailed quantitative information; however, this software has been exclusively used in animal experimental models, including rodents. Therefore, in this report, we introduced 3D quantitative analyses of the alveolar bone before and after orthodontic treatment to evaluate the morphological condition of the alveolar bone in humans.

We selected this patient because inflammation, swelling, and recession in the gingiva are sometimes known to occur in patients with a high-displaced canine,

especially in old age. The patient described in this report was 60 years and 1 month old before treatment. In this case, we analyzed the alveolar bone before and after orthodontic treatment by using a 3D structural analysis software for evaluating the morphological condition of the bone. Interestingly, the cortical bone did not show any sign of recovery unlike the trabecular bone (Figures 3C and 4C). This may be because the trabecular bone was affected easily within a short period, while the cortical bone was less affected, as shown in previous osteoporotic models.<sup>20,21</sup> Furthermore, a recent study suggested that the cortical bone and trabecular bone did not show the same response in osteopenia.<sup>22</sup> If a reference phantom was simultaneously scanned when the data were acquired, bone mineral density analysis could be performed to obtain further information.<sup>23,24</sup>

Studies have reported that the marrow space star volume is a bone structural parameter that can reveal trabecular connectivity.<sup>17-19</sup> Some reports have documented the marrow space star volume of the lumbar vertebra and iliac crest, and have compared the data, for example, before/after treatment. However, few studies have analyzed the alveolar bone. Therefore, future studies investigating and comparing the marrow space star volume in the alveolar bone of patients might yield interesting results.

When planning treatment using dental implants, CBCT data are now essential to obtain detailed information on the size of the alveolar bone and the location of the mandibular canal or maxillary sinus floor before implant surgery.<sup>25,26</sup> Likewise, in the orthodontic field, detailed information on the alveolar bone condition around the tooth prior to treatment is helpful in preventing gingival recession and/or relapse.

## CONCLUSION

In conclusion, 3D structural analysis to evaluate the morphological condition of a bone may be useful in a selected group of patients.

## REFERENCES

1. Newman WG. Possible etiologic factors in external root resorption. *Am J Orthod* 1975;67:522-39.
2. Fuss Z, Tsesis I, Lin S. Root resorption--diagnosis, classification and treatment choices based on stimulation factors. *Dent Traumatol* 2003;19:175-82.
3. Ishida Y, Kanno Z, Soma K. Occlusal hypofunction induces atrophic changes in rat gingiva. *Angle Orthod* 2008;78:1015-22.
4. Enokida M, Kaneko S, Yanagishita M, Soma K. Influence of occlusal stimuli on the remodelling of alveolar bone in a rat hypofunction-recovery model. *J Oral Biosci* 2005;47:321-34.
5. Shimomoto Y, Chung CJ, Iwasaki-Hayashi Y, Muramoto T, Soma K. Effects of occlusal stimuli on alveolar/jaw bone formation. *J Dent Res* 2007;86:47-51.
6. Shimizu Y, Hosomichi J, Kaneko S, Shibutani N, Ono T. Effect of sympathetic nervous activity on alveolar bone loss induced by occlusal hypofunction in rats. *Arch Oral Biol* 2011;56:1404-11.
7. Shimizu Y, Hosomichi J, Nakamura S, Ono T. Micro-computed tomography analysis of changes in the periodontal ligament and alveolar bone proper induced by occlusal hypofunction of rat molars. *Korean J Orthod* 2014;44:263-7.
8. Shimizu Y, Ishida T, Hosomichi J, Kaneko S, Hatano K, Ono T. Soft diet causes greater alveolar osteopenia in the mandible than in the maxilla. *Arch Oral Biol* 2013;58:907-11.
9. Castro LO, Castro IO, de Alencar AH, Valladares-Neto J, Estrela C. Cone beam computed tomography evaluation of distance from cemento-enamel junction to alveolar crest before and after nonextraction orthodontic treatment. *Angle Orthod* 2016;86:543-9.
10. Ann HR, Jung YS, Lee KJ, Baik HS. Evaluation of stability after pre-orthodontic orthognathic surgery using cone-beam computed tomography: A comparison with conventional treatment. *Korean J Orthod* 2016;46:301-9.
11. Choi JH, Park CH, Yi SW, Lim HJ, Hwang HS. Bone density measurement in interdental areas with simulated placement of orthodontic miniscrew implants. *Am J Orthod Dentofacial Orthop* 2009;136:766.e1-12.
12. Renkema AM, Sips ET, Bronkhorst E, Kuijpers-Jagtman AM. A survey on orthodontic retention procedures in The Netherlands. *Eur J Orthod* 2009;31:432-7.
13. van Leeuwen EJ, Maltha JC, Kuijpers-Jagtman AM, van't Hof MA. The effect of retention on orthodontic relapse after the use of small continuous or discontinuous forces. An experimental study in beagle dogs. *Eur J Oral Sci* 2003;111:111-6.
14. Reitan K. Tissue rearrangement during retention of orthodontically rotated teeth. *Angle Orthod* 1959;29:105-13.
15. Edwards JG. A long-term prospective evaluation of the circumferential supracrestal fiberotomy in alleviating orthodontic relapse. *Am J Orthod Dentofacial Orthop* 1988;93:380-7.
16. Bouxsein ML, Boyd SK, Christiansen BA, Guldborg RE, Jepsen KJ, Müller R. Guidelines for assessment of bone microstructure in rodents using micro-computed tomography. *J Bone Miner Res* 2010;25:

- 1468-86.
17. Vesterby A. Marrow space star volume can reveal change of trabecular connectivity. *Bone* 1993;14:193-7.
  18. Vesterby A. Star volume of marrow space and trabeculae in iliac crest: sampling procedure and correlation to star volume of first lumbar vertebra. *Bone* 1990;11:149-55.
  19. Kazama JJ, Koda R, Yamamoto S, Narita I, Gejyo F, Tokumoto A. Cancellous bone volume is an indicator for trabecular bone connectivity in dialysis patients. *Clin J Am Soc Nephrol* 2010;5:292-8.
  20. Aoki K, Saito H, Itzstein C, Ishiguro M, Shibata T, Blaque R, et al. A TNF receptor loop peptide mimic blocks RANK ligand-induced signaling, bone resorption, and bone loss. *J Clin Invest* 2006;116:1525-34.
  21. Sato K, Suematsu A, Nakashima T, Takemoto-Kimura S, Aoki K, Morishita Y, et al. Regulation of osteoclast differentiation and function by the CaMK-CREB pathway. *Nat Med* 2006;12:1410-6.
  22. Simsek Kiper PO, Saito H, Gori F, Unger S, Hesse E, Yamana K, et al. Cortical-bone fragility--insights from sFRP4 deficiency in Pyle's disease. *N Engl J Med* 2016;374:2553-62.
  23. Oishi S, Shimizu Y, Hosomichi J, Kuma Y, Nagai H, Maeda H, et al. Intermittent hypoxia induces disturbances in craniofacial growth and defects in craniofacial morphology. *Arch Oral Biol* 2016;61:115-24.
  24. Oishi S, Shimizu Y, Hosomichi J, Kuma Y, Maeda H, Nagai H, et al. Intermittent hypoxia influences alveolar bone proper microstructure via hypoxia-inducible factor and VEGF expression in periodontal ligaments of growing rats. *Front Physiol* 2016;7:416.
  25. Ito K, Gomi Y, Sato S, Arai Y, Shinoda K. Clinical application of a new compact CT system to assess 3-D images for the preoperative treatment planning of implants in the posterior mandible A case report. *Clin Oral Implants Res* 2001;12:539-42.
  26. Nomura Y, Watanabe H, Honda E, Kurabayashi T. Reliability of voxel values from cone-beam computed tomography for dental use in evaluating bone mineral density. *Clin Oral Implants Res* 2010;21:558-62.